GLOBAL ANALYSIS OF MASS TRANSFER CYCLES IN CATACLYSMIC VARIABLES

A. R. King, [1], J. Frank, [2] U. Kolb [1,3,4] and H. Ritter [4]

ABSTRACT

We give a global analysis of mass transfer variations in CVs. We show that limit cycles driven by variations of the secondary star's radius alone require this radius to be sensitive to the instantaneous mass transfer rate. The only promising mechanism for this is irradiation of the secondary by the accreting primary. Explicit modelling of this process shows however that cycles do not occur for secondary masses $\lesssim 0.65 M_{\odot}$. For such masses, the thermal inertia of the convective envelope is so large that irradiation cannot expand it relative to the Roche lobe, and the system finds a stable mass transfer rate. In constrast large–amplitude limit cycles occur for all secondary masses if the angular momentum losses from the binary are assumed to increase rather modestly with the mass transfer rate simultaneously with the radius variations.

Subject headings: accretion — instabilities — stars: binaries: close — stars: cataclysmic variables —

[1] Astronomy Group, University of Leicester, Leicester LE1 7RH, U.K. (ark@star.le.ac.uk, uck@star.le.ac.uk)

[2] Department of Physics and Astronomy, Louisiana State University, Baton Rouge, LA 70803-4001, USA (frank@rouge.phys.lsu.edu)

[3] UCO/Lick Observatory, Board of Studies in Astronomy and Astrophysics, UCSC, Santa Cruz, CA 95064, USA

[4] Max–Planck–Institut für Astrophysik, Karl–Schwarzschild–Str. 1, D 85748 Garching, Germany (hsr@MPA-Garching.MPG.DE)

1. INTRODUCTION

It is by now widely accepted that the evolution of cataclysmic variables (CVs) is driven by orbital angular momentum losses (see e.g. King, 1988 for a review). In this picture most properties of the binary, particularly the mass transfer rate, depend essentially only on the secondary mass M_2 and change on the timescale $t_J \sim 10^8 - 10^9$ yr for angular momentum loss. Since the evolution depends only weakly on the white dwarf mass M_1 this is equivalent to postulating a fairly tight relation between the transfer rate $-\dot{M}_2$ and the binary period P. Mass transfer rates inferred from observation (e.g. Patterson, 1984, Warner, 1987) do not conform to this postulate, and indeed show a rather wide spread at any given period: this is probably the reason that CV subtypes with very different features can have similar periods. To resolve the apparent discrepancy between this inferred spread and the evolutionary calculations, one notes that the latter predict only the secular mean mass transfer rate, i.e. the rate averaged over times long compared with the time t_L on which the Roche lobe moves through a stellar scale height H. Since H is typically only $\sim 10^{-4}$ of the stellar radius R_2, we have $t_L \sim (H/R_2)t_J \sim 10^4 - 10^5$ yr. The transfer rate can fluctuate strongly about the secular mean value on timescales $>> t_L$ but $<< t_J$ without upsetting the basic evolutionary picture. Such fluctuations would not of course be directly observable, and would naturally produce a range of instantaneous mass transfer rates at each period. Moreover they would determine the relation of each CV subtype to the others: in some sense these must all represent various phases of the mass transfer cycles at a given period.

While this picture has a certain plausibility, we still do not know if these cycles really exist, let alone their nature. We have investigated these questions in a series of papers (Ritter et al, 1995, 1996b; King, 1995; King et al 1995). It appears that irradiation of the companion star by the accretion flow on to the white dwarf is central to the process. However, we currently have no comprehensive picture of it, and it still seems possible that other effects may play a role.

The aim of this paper is to provide a general framework for studying mass transfer variations in a model–independent way. This allows us to perform a global analysis of these variations and look for the conditions under which limit–cycle behaviour occurs. By identifying the properties required for such cycles, we hope to narrow down the search for the physical mechanism(s) driving them. We establish that limit cycles can result from variations of the stellar radius alone only if the latter is sensitive to the instantaneous mass transfer rate. While we briefly consider other possibilities, the most immediately plausible way in which such a dependence can arise is through irradiation by the accreting component. However, explicit modelling of the effects of irradiation shows that limit cycles driven by radius variations alone are too restricted in occurrence to explain CV mass transfer variations. This problem is resolved if we also assume that the angular momentum losses increase rather modestly with the transfer rate. It appears that the thermal inertia of the convective envelope of the irradiated companion supplies the hysteresis required for a cycle, while the enhanced angular momentum losses prevent the system stabilizing at a steady mass transfer rate.

2. GLOBAL ANALYSIS OF MASS TRANSFER VARIATIONS

In this section we cast the equations governing time–dependent mass transfer in a semi–detached binary in a form suitable for global analysis. We restrict ourselves here to studying the effect of variations in the radius R_2 of the lobe–filling star on the transfer rate as this is the simplest way of causing mass transfer variations. However our results are easily generalized to include other forms of variation, and we give an example in Sect. 6 below.

Radius changes can result from dynamical, thermal or secular processes. For example, local adjustments in the structure of the atmospheric layers can take place on the shortest (dynamical) timescale, while adjustments of the stellar radius in response to secular mass loss occur on the longest (secular) timescale t_J. Here we are interested in phenomena that occur on intermediate timescales, so that the effects of rapid variations are averaged out and secular variations can be neglected. We represent the radius variation as

$$\frac{\dot{R}_2}{R_2} = \zeta_s \frac{\dot{M}_2}{M_2} + K(R_2, \dot{M}_2) \, . \tag{1}$$

Here ζ_s is the adiabatic mass–radius exponent ($\simeq -1/3$ for a fully convective star) and $K(R_2, \dot{M}_2)$ represents all radius variations other than the adiabatic reaction to mass loss (e.g. thermal relaxation, nuclear evolution, or irradiation of the star by the primary). For the moment we do not specify $K(R_2, \dot{M}_2)$, but instead attempt to discover what form it must have in order to produce the mass transfer rate variations whose existence we have inferred. Explicit examples of K are discussed in Sect. 3 and 5. The change of the mass transfer rate is given by

$$\ddot{M}_2 = \frac{\dot{M}_2}{H}(\dot{R}_2 - \dot{R}_{\rm L}) \approx \dot{M}_2 \frac{R_2}{H}\left(\frac{\dot{R}_2}{R_2} - \frac{\dot{R}_{\rm L}}{R_{\rm L}}\right) \, , \tag{2}$$

where $R_{\rm L}$ is the critical Roche radius, and H is the pressure scale height in the secondary star's atmosphere. The approximation given by (2) is justified since in all cases of interest $|R_2 - R_{\rm L}| << R_{\rm L}, R_2$. The response of the Roche radius to mass loss is described by

$$\frac{\dot{R}_{\rm L}}{R_{\rm L}} = \zeta_{\rm R} \frac{\dot{M}_2}{M_2} + 2\frac{\dot{J}}{J} \, , \tag{3}$$

where $\zeta_{\rm R}$ is a function of the mass ratio M_2/M_1, approximately given by $\zeta_{\rm R} \approx 2M_2/M_1 - 5/3$ for conservative mass transfer, and $\dot{J}$ is the rate of loss of orbital angular momentum. Inserting (1) and (3) into (2), we obtain

$$\ddot{M}_2 = \dot{M}_2 \frac{R_2}{H}\left((\zeta_s - \zeta_{\rm R})\frac{\dot{M}_2}{M_2} + K - 2\frac{\dot{J}}{J}\right) \, . \tag{4}$$

Equations (1) and (4) are our basic equations which we now cast into a more suitable dimensionless form. We introduce the timescale for secular orbital angular momentum losses

$$t_J = -\frac{J}{\dot{J}} \, , \tag{5}$$

which is typically $\sim 10^8 - 10^9$ yr, and we define a dimensionless mass transfer rate

$$x = -\frac{\dot{M}_2}{M_2}(\zeta_s - \zeta_{\rm R})\frac{t_J}{2} = \frac{-\dot{M}_2}{M_2/D_s t_J} \, , \tag{6}$$

where $D_s = \frac{1}{2}(\zeta_s - \zeta_{\rm R})$. Thus x is the mass transfer rate in units of the adiabatic mass transfer rate. A system undergoing stable mass transfer may be expected to do so at $x \sim 1$ (see Sect. 3). We also introduce the dimensionless stellar radius

$$r = R_2/R_e \, , \tag{7}$$

where $R_e = R_e(M_2)$ is the radius of the secondary in thermal equilibrium for a given mass, i.e. the main–sequence radius if the secondary is an unevolved hydrogen–rich star. As we discuss in Sect. 3, the secular equilibrium radius of the companion under stable mass transfer is slightly different from R_e. Although the equilibrium radius R_e is only defined in absence of mass transfer, we write formally

$$\frac{\dot{R}_e}{R_e} = \zeta_e \frac{\dot{M}_2}{M_2} , \tag{8}$$

where $\zeta_e > 0$ is the thermal equilibrium mass–radius exponent. From (6), and neglecting secular variations of H, it is easy to show that

$$-\ddot{M}_2 = \frac{M_2}{D_s t_J}\dot{x} + \frac{\dot{M}_2 x}{D_s t_J} + \dot{M}_2 \frac{\mathrm{d}\ln{(D_s t_J)}}{\mathrm{d}t} . \tag{9}$$

Finally, we introduce $\epsilon = H/R_e$, which is typically $\simeq 10^{-4}$ (Ritter 1988). We define the dimensionless thermal relaxation function $p(r,x) = \frac{1}{2}K t_J$, and the dimensionless time $\tau = 2t/(\epsilon t_J)$. With these assumptions and definitions (9) becomes

$$\frac{\mathrm{d}x}{\mathrm{d}\tau} = rx[1+p(r,x)-x] + \frac{\epsilon x}{2}\left[\frac{x}{D_s} + \frac{\mathrm{d}\ln{(D_s t_J)}}{\mathrm{d}(t/t_J)}\right]. \tag{10}$$

Note that since the terms inside the second set of square brackets are of order unity and they are multiplied by ϵ, they can be safely neglected. Thus (10) reduces to

$$\frac{\mathrm{d}x}{\mathrm{d}\tau} = rx[1+p(r,x)-x] . \tag{11}$$

With the same conventions, the radius equation (1) becomes

$$\frac{\mathrm{d}r}{\mathrm{d}\tau} = \epsilon r\left[p(r,x) - \frac{x}{\lambda}\right] , \tag{12}$$

where $\lambda = 2D_s/(\zeta_s - \zeta_e) = (\zeta_s - \zeta_\mathrm{R})/(\zeta_s - \zeta_e)$. We note that for systems which are dynamically stable against mass transfer (i.e. for which $D_s > 0$), we have $\lambda \gtrless 0$ if $\zeta_s - \zeta_e \gtrless 0$. We recall that ζ_s describes the behaviour of stars under rapid (adiabatic) mass loss and that $\zeta_s - \zeta_e$ changes sign at $M_2 \approx 0.75\mathrm{M}_\odot$ (Hjellming 1989).

The equations (11) and (12) derived above describe deviations from secular mean values, provided that these evolve on timescales shorter than t_J but long enough for any dynamical variations to average out. In the absence of such fluctuations on intermediate timescales, the system will settle at the stationary point(s) of these equations. These are found by setting $\mathrm{d}r/\mathrm{d}\tau = \mathrm{d}x/\mathrm{d}\tau = 0$, giving an explicit solution for the secular mass transfer rate

$$x_0 = \frac{\lambda}{\lambda - 1} = \frac{\zeta_s - \zeta_\mathrm{R}}{\zeta_e - \zeta_\mathrm{R}} , \tag{13}$$

and an implicit expression for the secular equilibrium radius

$$p_0 = p(r_0, x_0) = \frac{1}{\lambda - 1} = \frac{\zeta_s - \zeta_e}{\zeta_e - \zeta_\mathrm{R}} , \tag{14}$$

which can in principle be solved for r_0 once an explicit expression for $p(x,r)$ is chosen (see Sect. 3 and 5).

We expect that deviations from quasi–steady mass transfer will decay on rather short timescales $t_{\rm L} = \epsilon t_J \sim 10^4 - 10^5$yr provided that no further perturbation occurs. Thus given the form of K, the behaviour of the system is simple to describe if the stationary points are stable. However, as we have anticipated in a previous paper (King et al, 1995) the interesting possibility of limit cycle behaviour arises if the stationary point(s) are unstable and satisfy some additional requirements discussed in Sect. 4.

3. SECULAR EVOLUTION

As a first application of the use of the formalism of the previous section we show here how a simple form for the radius variation function K yields estimates for the secular equilibrium radius and mass transfer rate, and allows a simple description of the evolution. We assume that the companion, if disturbed, attempts to return to its equilibrium radius on a Kelvin–Helmholtz timescale, and write

$$K(R_2, \dot{M}_2) = -\frac{f}{t_{\rm KH}} \frac{(R_2 - R_e)}{R_e} \; , \tag{15}$$

where f is a dimensionless factor depending on the structure of the companion, and $t_{\rm KH}$ is the Kelvin–Helmholtz timescale for the equilibrium model. With the units and definitions adopted earlier, this implies

$$p(r, x) = -\frac{f\rho}{2}(r - 1) \; . \tag{16}$$

where $\rho = t_J/t_{\rm KH}$ is the ratio of timescales ($\rho \approx 0.2$ for values of M_2 just above the gap and $\rho \sim 10$ for $M_2 = 1{\rm M}_\odot$ under typical driving rates). The secular mass transfer rate is given as before by (13), and using (16) in (14), we can solve for the secular equilibrium radius, obtaining

$$r_0 = 1 + \frac{\zeta_e - \zeta_s}{\zeta_e - \zeta_{\rm R}} \frac{2}{f\rho} \; . \tag{17}$$

We see from (13, 17) that the signs of $x_0 - 1, r_0 - 1$ both depend on $\zeta_e - \zeta_s$ alone since $\zeta_e - \zeta_{\rm R} > 0$ for all cases of interest. If the companion is largely convective, so that it tends to expand on mass loss ($\zeta_s < 0$), then clearly $\zeta_e > \zeta_s$, $x_0 < 1$ and $r_0 > 1$, i.e. the star is slightly larger than the equilibrium radius and transfers mass at a rate slightly below the adiabatic value. The converse is true when $M_2 \gtrsim 0.75{\rm M}_\odot$ since then $\zeta_s > \zeta_e$, i.e. the companion tends to shrink upon rapid mass loss faster than its equilibrium radius. Note that the correction to the radius is of order $t_{\rm KH}/ft_J$, while the secular mass transfer rate becomes

$$(-\dot{M}_2)_{\rm sec} = \frac{2M_2}{(\zeta_e - \zeta_{\rm R})t_J} \; . \tag{18}$$

For stable mass transfer we have $\zeta_s - \zeta_{\rm R} > 0$ and $\zeta_e - \zeta_{\rm R} > 0$; and (18) together with (3) implies that $\dot{R}_{\rm L}/R_{\rm L} = -2t_J^{-1}\zeta_e/(\zeta_e - \zeta_{\rm R})$, while the binary shrinks and evolves to shorter periods on a timescale $\sim t_J$. Furthermore it is easy to show from (7), (8), and (18) that $\dot{R}_{\rm L}/R_{\rm L} = \dot{R}_2/R_2 = \dot{R}_e/R_e$ under stable secular evolution as expected. We discuss the stability of this type of evolution below in the next section.

The secular equilibrium radius and mass transfer rate depend only on the angular momentum losses (t_J) and the mass of the companion, and are independent of the details of the preceding evolution. Since t_J is only weakly dependent on the primary mass, it can be regarded as a function of M_2 alone to a good approximation. Thus systems that start from a variety of initial conditions and come into contact at different periods will nevertheless follow the same evolutionary path once they reach secular equilibrium. So, for example, on a period–mass or radius–mass diagram all CV systems with $M_2 \lesssim 0.75\mathrm{M}_\odot$ follow an evolutionary path slightly above the main sequence locus. In the usual disrupted–braking picture (e.g. King, 1988) they all detach at (almost) the same period, return to contact at (almost) the same period and eventually reach (almost) the same period minimum. Similar conclusions were reached by Stehle, Ritter & Kolb (1996) using a more detailed treatment.

4. PHASE PLANE ANALYSIS

The last section showed how a simple form of the radius variation function K or p gives the fixed points of the system. Our main aim in this paper is to find forms of this function that produce limit cycle behaviour.

4.1. Mathematical Treatment

Given any form of p, the global behaviour of the system (such as the presence of limit cycles, etc) is determined largely by the stability properties of the fixed points. Accordingly we consider small deviations Δr, Δx from r_0, x_0, and linearize (10, 12) about them. We keep the extra term in (10) for completeness: it turns out not to be important except in those relatively rare cases where lower order terms cancel each other. Retaining only terms up to first order in ϵ this gives

$$\dot{\Delta r} = \alpha_{11}\Delta r + \alpha_{12}\Delta x \ , \tag{19}$$

$$\dot{\Delta x} = \alpha_{21}\Delta r + \alpha_{22}\Delta x \ , \tag{20}$$

where the dot denotes differentiation wrt τ, and

$$\alpha_{11} = \epsilon r_0 p_r \ , \tag{21}$$

$$\alpha_{12} = \epsilon r_0 (p_x - 1/\lambda) \ , \tag{22}$$

$$\alpha_{21} = r_0 x_0 p_r - \epsilon \frac{x_0}{r_0}\left[\frac{x_0}{2D_s} + \frac{\mathrm{d}\ln(D_s t_J)}{2\mathrm{d}(t/t_J)}\right] , \tag{23}$$

$$\alpha_{22} = r_0 x_0 (p_x - 1) + \epsilon x_0/2D_s \ , \tag{24}$$

where p_x, p_r are the partial derivatives of p wrt x, r, and all quantities are evaluated at (r_0, x_0). Cross–eliminating, it is easy to show that both Δr and Δx obey a second order constant–coefficient equation of the form

$$\ddot{y} + 2\alpha\dot{y} + \omega^2 y = 0 \ , \tag{25}$$

with $\alpha = -(1/2)\mathrm{trace}(\alpha_{ij})$, $\omega^2 = \det(\alpha_{ij})$, or

$$2\alpha = r_0 x_0 (1 - p_x) - \epsilon(x_0/2D_s + r_0 p_r) \ , \tag{26}$$

$$\omega^2 = -\epsilon r_0^2 p_r \ . \tag{27}$$

In (27) we have used (13) and (6) to eliminate x_0, and dropped terms $O(\epsilon^2)$ and higher. Seeking solutions of (25) of the form $e^{\sigma\tau}$ gives $\sigma = -\alpha \pm \sqrt{\alpha^2 - \omega^2}$. This allows us to classify the fixed points according to the signs of α, ω^2 and the sign of the discriminant $\alpha^2 - \omega^2$. Since

$\alpha^2 \geq 0$ we must have $\omega^2 \geq 0$ if the discriminant is ≤ 0. This leads to the possibilities listed in Table 1.

The character of each case is revealed by the corresponding trajectories in the (r, x) plane. The trajectories are bounded, giving a stable fixed point, if $\alpha > 0$, and diverge to infinity if $\alpha < 0$. The trajectories are quasiperiodic if $\omega^2 > 0$ and aperiodic otherwise. Thus trajectories around a stable (unstable) focus spiral inward (outward) as $\tau \to \infty$, corresponding to damped or growing (i.e. overstable) oscillations of the transfer rate around the secular mean respectively. Trajectories around a node correspond to overcritically damped or antidamped behaviour of the transfer rate. Hence these trajectories do not complete a full revolution before reaching the fixed point from infinity (damped case) or diverging to infinity (antidamped case). The kind of fixed point called a center in Table 1 is neutrally stable, the trajectories being concentric ellipses; in practice its character will be determined by the higher order terms neglected in the linearization, and the resultant point will be a stable or unstable weak focus. The trajectories around a saddle point are hyperbolic, and this fixed point is evidently always unstable. These behaviours can also be inferred directly from the original perturbation equations (19, 20) by noting how the signs of $\dot{\Delta r}, \dot{\Delta x}$ change as the system point crosses the curves $\dot{\Delta r} = 0, \dot{\Delta x} = 0$. Fig. 1 shows two generic examples of the local behaviour of the solutions near the fixed point. As can be seen, the curves $\dot{\Delta r} = 0, \dot{\Delta x} = 0$ divide the (r, x) plane near the fixed point into four regions. The signs of the α_{ij} then fix the signs of $\dot{\Delta r}, \dot{\Delta x}$ in each of these regions, causing the system point to move as indicated by the arrows in each region as τ increases. In one case the result is an unstable focus (Fig. 1a), and in the other case we have hyperbolic trajectories around a saddle point (Fig. 1b). A treatment on these lines is given by King (1995).

We can now examine the stability of the simple secular evolution model of CVs without irradiation discussed in the previous section. In this case the dimensionless radius variation function (16) is independent of the mass transfer rate, i.e. $p_x = 0$. Furthermore one can show easily that

$$p_r(x_0, r_0) = \left.\frac{\partial p}{\partial r}\right|_{x_0, r_0} = -\frac{f t_J}{2 t_{\rm KH}} , \tag{28}$$

and thus from (26) that

$$2\alpha = r_0 x_0 - \epsilon\left(\frac{x_0}{2D_s} + r_0 p_r\right) \approx r_0 x_0 = \frac{\zeta_s - \zeta_{\rm R}}{\zeta_e - \zeta_{\rm R}}\left(1 + \frac{\zeta_e - \zeta_s}{\zeta_e - \zeta_{\rm R}}\frac{2}{f\rho}\right) . \tag{29}$$

For dynamically and thermally stable systems both $\zeta_s - \zeta_{\rm R}$ and $\zeta_e - \zeta_{\rm R}$ are positive implying

Table 1: Classification of Fixed Points

Discriminant	*Determinant*	$-\frac{1}{2}$ *Trace*	*Type of Fixed Point*
$\alpha^2 - \omega^2 < 0$	$\omega^2 > 0$	$\alpha > 0$	Stable Focus
		$\alpha = 0$	Center
		$\alpha < 0$	Unstable Focus
$\alpha^2 - \omega^2 = 0$	$\omega^2 > 0$	$\alpha > 0$	Stable Node
		$\alpha < 0$	Unstable Node
$\alpha^2 - \omega^2 > 0$	$\omega^2 > 0$	$\alpha > 0$	Stable Node
		$\alpha < 0$	Unstable Node
	$\omega^2 < 0$		Saddle

$\alpha > 0$. From (27) one obtains

$$\omega^2 = \epsilon \frac{f\rho}{2}\left(1 + \frac{\zeta_e - \zeta_s}{\zeta_e - \zeta_{\rm R}}\frac{2}{f\rho}\right)^2 , \tag{30}$$

which is positive always and thus ω is real. Referring to Table 1, one sees that the evolution of "ordinary" CVs without irradiation of the companion is always stable. The character of the fixed point depends on the sign of $\alpha^2 - \omega^2$ and it is a stable node in most cases of interest. As explained in the Introduction, in this paper we are primarily interested in the possibility of medium–term cycles in the mass transfer rate. Formally this means that we seek limit–cycle solutions of the governing equations (11, 12), corresponding to closed trajectories in the (r, x) plane. A necessary (but not sufficient) condition for limit cycles is that the Poincaré index of the fixed point should be +1 (e.g. Minorsky 1962). This is just another way of saying that if we move successively through the four regions on Fig. 1, the pattern of arrows on the figure must rotate precisely once, in the same sense as our motion around the fixed point. This condition rules out saddle points, so we require $\omega^2 > 0$. From the Poincaré–Bendixson theorem (e.g. Glendinning 1994) we know that such trajectories give limit cycles only if they enclose an unstable fixed point; thus we need $\alpha < 0$, $\omega^2 > 0$ at this point. The behaviour of the system as it diverges from this point is determined by the form of the curves $\dot r = 0$, $\dot x = 0$. In practice for the system (11, 12) the sharp difference in timescales for motions towards the two curves means that only the curve $\dot x \propto -\ddot M_2 = 0$ is important: the system point moves almost vertically back to this curve if removed from it (the only exception to this is if $-\dot M_2$ tends to zero, which occurs exponentially slowly – see e.g. King 1995 and below). Physically this corresponds to the fact that very large changes in the transfer rate $-\dot M_2$ result from modest motions of the stellar radius of order the scale height H. For $x \neq 0$ the equation $\dot x = 0$ (cf eq. 11) is

$$1 + p(r, x) - x = 0 . \tag{31}$$

At points (r, x) on this curve

$$\frac{{\rm d}x}{{\rm d}r} = \frac{p_r}{1 - p_x} = \frac{-\omega^2 x_0}{2\alpha r_0 \epsilon} + O(\epsilon) , \tag{32}$$

where the second equality holds at the fixed point. With $\omega^2 > 0$ we see that the sign of ${\rm d}x/{\rm d}r$ is given by that of $-\alpha$. Thus the fixed point is stable if it occurs on a branch of the curve $\dot x = 0$ where ${\rm d}x/{\rm d}r < 0$, but is unstable if ${\rm d}x/{\rm d}r > 0$ at this point. Limit–cycle behaviour requires an unstable fixed point so that the system cannot settle there, but also that the system cannot escape from a neighborhood of this point. Away from the curve $\dot x = 0$ the system point moves almost vertically, so this confinement is effectively only required towards small and large x. The former is assured, since the line $x = 0$ is reached exponentially slowly; thus limit cycles must occur provided only that there is an attracting branch of the curve $\dot x = 0$ available vertically above the intersection. As can be seen from Fig. 2, these requirements amount to demanding that the $\dot x = 0$ curve should have positive slope where it intersects $\dot r = 0$, and bend back to a negative slope above this intersection. The forms of $p(r, x)$ we shall consider give curves $\dot x = 0$ of this type. The directions of the vertical arrows in the Fig. 2 show that the upper branch (with ${\rm d}x/{\rm d}r < 0$) is an attractor. On this branch AB the system moves to larger r, decreasing x also. In physical terms the K or $p(r, x)$ function is increasing the relative stellar radius r here, i.e. the actual stellar radius relative to the corresponding equilibrium radius R_e. This is competing with the simultaneous expansion of the Roche lobe relative to R_e, which must be occurring as the mass transfer rate x is above the secular mean value x_0 represented by the fixed point. Ultimately at point B, the relative radius expansion becomes too slow compared with that of the Roche lobe to sustain the large mass transfer rate which in turn drives the radius expansion. This is inevitable since the system cannot remain indefinitely above the secular mean transfer rate. The reduced transfer rate near B further decreases the relative radius expansion, hence dropping x still more: this negative feedback causes the transfer rate to fall rapidly (timescale ϵt_J) to very low values in a nearly detached state (B $\rightarrow$ C). The system does not reach $x = 0$ because this would take an infinite time, but meanwhile moves to smaller r (C $\rightarrow$ D) because the $p(r,x)$ term is no longer supporting the secondary's increased size. Once the system crosses the curve $\dot{x} = 0$, x begins to increase because the Roche lobe is now shrinking more rapidly than the star, until finally at D positive feedback makes the system point move rapidly (timescale ϵt_J) upwards to the attracting branch at A, and the cycle restarts. The timescales in the high and low states depend on the detailed form of $p(r,x)$, while transitions between these states have typical time ϵt_J, as already stated.

4.2. Physical Interpretation

So far we have simply considered the mathematical requirements for a limit cycle, without any discussion of what physical processes might determine the right–hand sides of equations (11, 12) and thus drive such a cycle. However the requirement that the fixed point should be unstable gives a powerful clue. From (26, 27) we find

$$p_x = 1 - \frac{2\alpha}{r_0 x_0} + \frac{\omega^2}{r_0^2 x_0} - \frac{\epsilon}{2D_s r_0} \; . \tag{33}$$

Since $\epsilon << 1$, $r_0 \simeq 1$, and we require $x_0 > 0$ for dynamically stable mass transfer ($D_s > 0$), we see that a limit cycle ($\alpha < 0$, $\omega^2 > 0$) requires p_x to be positive definite, and indeed > 1. Thus no limit cycle is possible if p is independent of x, i.e. *the existence of mass transfer oscillations driven by radius variations requires a regime in which the variation function K depends on the mass transfer rate*, and moreover is an increasing function of it.

Although this is a necessary but certainly not sufficient condition, it is already strong enough to constrain the possible causes of limit cycles very severely. In looking for the causes of long–term cycles, we can assume that the secondary is always in hydrostatic equilibrium. Then radius changes beyond the adiabatic response can only result from nuclear evolution or thermal imbalance. The former can be excluded immediately, as not only is the timescale generally far too long for the required cycles, but it is irreversible rather than cyclic. This leaves us with thermal imbalance. The equations of stellar structure do not depend explicitly on $\dot{M}_2$, nor could such a dependence appear in the central boundary conditions. The only remaining possibility is that the outer boundary condition depends on $\dot{M}_2$ in such a way that the thermal structure of the star is perturbed. There is one fairly obvious way this might come about: the outer boundary condition may be significantly affected by irradiation by the accreting component.

We shall study irradiation in detail below, but we note that it is slightly indirect, i.e. the mass loss represented by $\dot{M}_2$ has to accrete on to the primary and produce radiation which is then intercepted by the secondary before this star is affected. We might ask if $\dot{M}_2$ can affect the thermal structure of the outer layers of the secondary more directly. Most simple ideas for doing this fail because mass is only lost from the star near L_1: most of the stellar surface experiences an extremely slow tangential flow. It seems unlikely that such a flow could radically affect the thermal structure of the star's outer layers, as it is probably close to thermal balance with the matter below. The Bernoulli effect reducing the pressure in this gas at a given height is not only very small, but actually decreases R_2 as $-\dot{M}_2$ increases, contrary to what is required. An apparently more promising idea is that the shear flow across the surface might promote magnetic activity in the star: if the stellar surface were increasingly covered by starspots, these would block the stellar radiation flux, and R_2 would grow on a thermal timescale. (Provided that the growth time of the starspots was much shorter than the latter timescale, the effect would actually be very similar to that of irradiation (see below): both cases invoke increased blocking of the stellar flux as the mass transfer rate rises, leading to thermal expansion of the star.) The main problem with this idea is the extremely slow flow velocity: it appears very unlikely that a highly subsonic shear flow would produce a significant increase in magnetic activity (Tout C.A. & Pringle J.E. 1992). This argument essentially forces us to conclude that *irradiation by the accreting primary star is the only promising mechanism for mass transfer cycles driven by radius variations.* We assumed this result in a recent paper (King et al., 1995). There we gave a simple analytic description of the reaction of the companion to weak irradiation and showed that the resulting radius variations drive limit cycle behaviour in at least some cases. In the next section we consider this process in more detail. Before doing so we note that we can extract some more information about the nature of the process driving the cycles from the condition that the system should on average be near the fixed point $\dot{R}_2 = 0, \ddot{M}_2 = 0$. From (1, 4) this implies

$$|K| \sim -\frac{\dot{J}}{J} \sim -\frac{\dot{M}_2}{M_2} \tag{34}$$

since ζ_s, ζ_R are $O(1)$. We shall see in the next section that irradiation works by blocking a fraction of the star's intrinsic luminosity, and K has a form such that

$$|K| \sim \frac{\Delta L R_2}{G M_2^2} \tag{35}$$

where ΔL is the irradiating luminosity. Combining (34, 35) we see that

$$\Delta L \sim \frac{G M_2(-\dot{M}_2)}{R_2} \sim \frac{M_2}{M_1}\frac{R_1}{R_2} L_{\rm accr} \sim 10^{-2} L_{\rm accr}, \tag{36}$$

where $L_{\rm accr}$ is the accretion luminosity. Thus the irradiation required to drive the cycles is only about 1% of the accretion luminosity. This is in good agreement with what we expect the secondary to absorb on geometrical grounds (it subtends a solid angle of a few percent at the primary star; and the absorption efficiency will be < 1). We note that for low–mass X–ray binaries, $R_1 \simeq 10^6$ cm, so (36) becomes $\Delta L \sim 10^{-5} L_{\rm accr}$, which does not agree well with what is likely to be absorbed by the secondary star.

5. SIMPLE MODELS WITH IRRADIATION

Here we shall apply the formalism worked out in the previous section and derive explicit expressions for p, p_r and p_x for two simple models with irradiation which we have used previously. The first model is the homologous model adopted by King et al. (1995), the second one the bipolytrope model used by Ritter et al. (1995, 1996b).

5.1. The irradiated homologous model

For describing the basic effects irradiation of the donor star has on the evolution of a CV, King et al. (1995) adopted a simple model for the reaction of a low-mass star to mass loss and irradiation, which is based on the following assumptions: 1) Homology relations can be used to describe the stellar structure, i.e. any stellar radius change is associated with a change of the surface and nuclear luminosity according to $L \propto R_2^2$ and $L_{\rm nuc} \propto R_2^{-3-\nu}$ ($\nu \simeq 6$), respectively, whereas the effective temperature T_* on the unirradiated portion of the stellar surface remains essentially constant. 2) If a fraction s of the stellar surface is exposed to a uniform irradiating flux F, the luminosity of the star, i.e. the loss of energy per unit time from the interior, is reduced by the blocking luminosity

$$L_b = sL \ \tanh\left\{k\, \frac{F}{F_*}\right\} , \tag{37}$$

where $F_* = \sigma T_*^4$ is the unperturbed stellar flux and k a free parameter of order unity which can be adjusted to approximate the results of more realistic model calculations (e.g. those by Ritter et al. (1995, 1996b)). The above ansatz for L_b is motivated by the facts that a) $L_b = 0$ if $F = 0$, b) $L_b \to sL$ if $F \gg F_*$, and c) that the transition between $F = 0$ and $F \gg F_*$ is smooth and monotonic. With these assumptions one obtains (cf. Eq.(8) of King et al. 1995)

$$p(r,x) = -\frac{f\rho}{2}\ \left\{\left[1 - s\ \tanh\left(\frac{x}{x_c}\right)\right]\ r^3 - r^{-(\nu+2)}\right\} , \tag{38}$$

where f is a constant (as in (15) but with a different value) which depends on the internal structure, i.e. the mass of the secondary, $\rho = t_J/t_{\rm KH}$ as before, and

$$x_c = \frac{2D_s\rho}{k\eta}\ \frac{M_2}{M_1}\ \frac{R_1}{R_e}\ \left(\frac{a}{R_e}\right)^2 \tag{39}$$

is the dimensionless, critical irradiation flux, typically $x_c \simeq 0.1\rho/\eta$. Here a is the orbital separation and η a dimensionless "efficiency factor" which relates the irradiating flux F to the mass transfer rate via

$$F = \frac{\eta}{8\pi}\ \frac{GM_1(-\dot M_2)}{R_1 a^2} . \tag{40}$$

From (38) we derive

$$p_r = -\frac{f\rho}{2}\ \left\{3\left[1 - s\ \tanh\left(\frac{x}{x_c}\right)\right]\ r^2 + (\nu+2)\, r^{-(\nu+3)}\right\} \tag{41}$$

and

$$p_x = \frac{sf\rho}{2x_c}\ r^3\ {\rm sech}^2\left(\frac{x}{x_c}\right) . \tag{42}$$

Taking (41) and (42) at the fixed point (r_0, x_0) and using (13) yields

$$p_r(r_0,x_0) = -\frac{f\rho}{2}\ \left\{3\left[1 - s\ \tanh\left(\frac{\zeta_s - \zeta_{\rm R}}{x_c(\zeta_e - \zeta_{\rm R})}\right)\right]\ r_0^2 + (\nu+2)\, r_0^{-(\nu+3)}\right\} \tag{43}$$

and

$$p_x(r_0,x_0) = \frac{sf\rho}{2x_c}\ r_0^3\ {\rm sech}^2\left(\frac{\zeta_s - \zeta_{\rm R}}{x_c(\zeta_e - \zeta_{\rm R})}\right) . \tag{44}$$

From (43) we see that $p_r < 0$ for $r_0 > 0$ and that, therefore, $\omega^2 > 0$. On the other hand, $p_x > 0$ for positive r_0 and x_0. The necessary condition for the occurrence of limit cycles, i.e. $\alpha < 0$ or $p_x > 1$, is equivalent to

$$2\frac{\zeta_s - \zeta_{\rm R}}{f\,r_0^3}\,\frac{t_{\rm KH}}{t_M} < 2s\,\frac{x_0}{x_c}\,{\rm sech}^2\left(\frac{x_0}{x_c}\right)\ , \tag{45}$$

where $t_M = D_s\,t_J/x_0 = (\zeta_e - \zeta_{\rm R})t_J/2$ is the mass transfer time scale at the fixed point.

Examining (45) we note that the left hand side does not depend on any assumptions about irradiation, but only on properties of the mean secular evolution (via $\zeta_s - \zeta_{\rm R}$, r_0 and t_M) and on the internal structure of the secondary (via ζ_s, ζ_e, f and $t_{\rm KH}$). In Fig. 3, discussed further in the next section, we plot the l.h.s. of (45) along a standard CV evolutionary sequence (e.g. from Kolb & Ritter 1992); in order to treat properly the thermal response of high–mass secondaries $M_2 \gtrsim 0.5{\rm M}_\odot$ with an extended radiative core the quantity f was replaced by $\mathcal{F}$, defined in (47) below. $\mathcal{F}$ scales roughly as $7M_2/3M_{ce}$, where M_{ce} is the mass of the convective envelope.

In contrast, the right hand side of (45) contains all the information about the irradiation model used, here in the form of the parameter s and the functional dependence on x_0. Most important is that, independent of any details about the efficiency of irradiation, the function $y\,{\rm sech}^2(y)$ has a maximum value Max $(y\,{\rm sech}^2(y)) \approx 0.45$ at $y \simeq 1$. We now assume one–sided irradiation ($s \simeq 0.5$), consistent with observations of a number of close binary central stars of planetary nebulae where the companion star clearly shows a hot, irradiated and a cool unlit hemisphere (for a list see Ritter, Zhang & Kolb 1996, in prep.). Then a comparison with Fig. 3 shows that condition (45) can be fulfilled only for $M_2 \gtrsim 0.6{\rm M}_\odot$, otherwise the fixed point is on a stable branch ($p_x < 1$) of the critical curve (31) and no limit cycles are possible. We shall recover this property also in the more realistic model below. Another way of expressing it is to note that (42) defines the value $x_{\rm turn}$ of the dimensionless transfer rate at the turning point $p_x = 1$ (cf (32) of the $\dot{x} = 0$ curve). For limit cycles we require x_0 to lie on the unstable ($p_x > 1$) part of this curve, i.e. we require $x_{\rm turn} > x_0$. The physical reason why this condition fails for $M_2 \lesssim 0.6{\rm M}_\odot$ is the sharp increase in the mass, and consequently thermal inertia, of the convective envelope at $M_2 \simeq 0.6{\rm M}_\odot$. Also working in the same direction is the fact that with decreasing stellar mass we have a lower internally generated stellar flux, which ultimately drives the expansion of the star. At lower masses this makes the K term too small to expand R_2 relative to the Roche lobe, as required to reach high transfer rates (A $\rightarrow$ B in Fig. 2). This behaviour is generic, and little affected by the detailed choice (38).

Selected examples of the integrations of equations (11) and (12) with $p(r,x)$ given by (38) are shown in Fig. 4. Case a represents a typical binary above the period gap with a critically damped stable behaviour whereas case b is an example of a system at somewhat longer period exhibiting limit cycles. Case c is marginally unstable according to (45) but its behaviour is determined by the higher order terms neglected in Sect. 4. Case d is also marginally unstable showing cycle behaviour with a relatively small amplitude.

5.2. The weakly irradiated bipolytrope model

In the following we shall use the bipolytrope approximation (e.g. Rappaport et al. 1983; Hameury et al. 1988; Kolb & Ritter 1992) for describing the internal structure of the donor star. Following Kolb & Ritter (1992) and using their notation we can write

$$K(R_2,\dot{M}_2) = \frac{R_2}{GM_2^2}\left[(L_{\rm nuc} - L)\,\mathcal{F}(Q,n_1) + L_{g_1}\,\frac{\partial H}{\partial Q}\,\frac{1}{H_2(Q,n_1)}\left\{\frac{\partial H}{\partial Q} + \frac{H}{f}\,\frac{\partial f}{\partial Q}\right\}^{-1}\right] \tag{46}$$

with

$$\mathcal{F}(Q,n_1) = \left\{ \frac{\partial H}{\partial Q} \frac{1}{H_2(Q,n_1)} + \frac{1}{f}\frac{\partial f}{\partial Q} \right\} \left\{ \frac{\partial H}{\partial Q} + \frac{H}{f}\frac{\partial f}{\partial Q} \right\}^{-1} . \tag{47}$$

Here $L_{\rm nuc}$ is the total nuclear luminosity of the star, L_{g_1}, n_1 and Q are respectively the gravothermal luminosity, the polytropic index and the relative radius $R_{\rm core}/R_2$ of the radiative core. $\mathcal{F}$ is a bipolytrope scaling factor which takes the approximate value $7M_2/3M_{ce}$. Note that in the preceding two equations and the rest of this subsection the symbols H and f have different meanings from those in the rest of the paper: $H = H(Q,n_1)$, $H_2(Q,n_1)$, and $f = f(Q,n_1)$ are dimensionless functions depending on the structure of the companion (see the above references for details).

For calculating the amount of luminosity L_b which is blocked by irradiating the star we adopt a point source model, i.e. we assume that the secondary is irradiated by a point source at the location of the white dwarf which has the accretion luminosity

$$L_{\rm accr} = \frac{GM_1(-\dot{M}_2)}{R_1} . \tag{48}$$

We further assume weak irradiation, i.e. that the vertical temperature gradient in the outermost layers of the star is much larger than the lateral temperature gradient. This is very reasonable in view of the estimate (36), which also agrees with what is expected on observational grounds. Then lateral energy transport can be neglected and the energy loss through any surface element of the irradiated parts of the star can be treated locally, i.e. as being independent of neighbouring surface elements. Thus the surface luminosity of the secondary can be written as

$$L = 4\pi R_2^2 \left\{ \frac{1}{2}(1+f_2)\,\sigma T_1^4 + \frac{1}{2}\int\limits_0^{\theta_{\rm max}} \left[\sigma T_2^4(\theta) - F(\theta)\right] \sin\theta \,{\rm d}\theta \right\} , \tag{49}$$

where T_1 denotes the effective temperature on the unirradiated parts of the star, $T_2(\theta)$ the (variable) effective temperature on the irradiated parts,

$$F(\theta) = \eta \frac{L_{\rm accr}}{4\pi a^2}\, h(\theta) \tag{50}$$

is the (variable) irradiating flux normal to the stellar surface and

$$h(\theta) = \frac{\cos\theta - f_2}{(1 - 2f_2\cos\theta + f_2^2)^{3/2}} . \tag{51}$$

Here θ is the colatitude of the surface element in question as measured from the substellar point, $\theta_{\rm max} = \arccos(f_2)$ the colatitude of the terminator (see Fig. 5 for a schematic representation of the geometry) and $f_2 = R_2/a$ the stellar radius in units of the orbital separation.

Introducing the dimensionless irradiating flux

$$y = \frac{F}{\sigma T_1^4} \tag{52}$$

and the function

$$G(y) = \frac{1}{\sigma T_1^4}\left[\sigma T_2^4 - F\right] = \left(\frac{T_2}{T_1}\right)^4 - y \tag{53}$$

we can now write

$$L = L_e r^2 \left\{ \frac{1}{2}(1+f_2) + \frac{1}{2} \int\limits_0^{\theta_{\max}} G(y(\theta)) \sin\theta \, \mathrm{d}\theta \right\} , \tag{54}$$

where $L_e = 4\pi\sigma R_e^2 T_1^4$ is the luminosity of the unirradiated star in thermal equilibrium. (54) has to be inserted in

$$p(r,x) = \frac{t_J}{2} K = \frac{t_J R_e}{2GM_2^2} r \left[(L_{\mathrm{nuc}} - L)\mathcal{F}(Q,n_1) + L_{g_1} \frac{\partial H}{\partial Q} \frac{1}{H_2(Q,n_1)} \left\{ \frac{\partial H}{\partial Q} + \frac{H}{f}\frac{\partial f}{\partial Q} \right\}^{-1} \right] . \tag{55}$$

Defining now

$$g(y) = -\frac{\mathrm{d}G}{\mathrm{d}y} = 1 - \frac{\mathrm{d}}{\mathrm{d}F(\theta)} \left(\sigma T_2^4(\theta) \right) \tag{56}$$

we find

$$\frac{\partial L}{\partial x} = -\eta \frac{M_2}{2D_s t_J} \left(\frac{R_2}{a} \right)^2 \frac{GM_1}{R_1} \int\limits_0^{\theta_{\max}} g(y(\theta))\, h(\theta) \sin\theta \, \mathrm{d}\theta , \tag{57}$$

and with (55)

$$p_x(r,x) = \frac{\eta}{4D_s} \frac{M_1}{M_2} \frac{R_e}{R_1} \left(\frac{R_e}{a} \right)^2 \mathcal{F}(Q,n_1)\, r^3 \int\limits_0^{\theta_{\max}} g(y(\theta))\, h(\theta) \sin\theta \, \mathrm{d}\theta . \tag{58}$$

Eliminating η by means of (48) and (50) yields

$$p_x(r,x) = \frac{1}{4D_s} \frac{t_M}{t_{\mathrm{KH}}} \mathcal{F}(Q,n_1)\, r^3 \int\limits_0^{\theta_{\max}} g(y(\theta))\, y(\theta) \sin\theta \, \mathrm{d}\theta . \tag{59}$$

Whereas the calculation of p_x is straightforward, at least to the extent that the only quantity which depends explicitly on x is L, the calculation of p_r cannot be done analytically because the dependence on r of the functions L_{nuc} and L_{g_1} is not known explicitly. However, it is clear that $p_r < 0$ because L_{nuc} scales with a rather large negative power of r, whereas roughly $L \sim r^2$ (see above, Sect. 5.1). Fig. 6 shows p_r obtained by numerical differentiation (with $Q =$ const.) along a standard CV evolutionary sequence (from Kolb & Ritter 1992).

The necessary condition for the occurrence of limit cycles, i.e. $\alpha < 0$ or $p_x(r_0, x_0) > 1$, is equivalent to

$$\Lambda \equiv 2 \frac{\zeta_s - \zeta_{\mathrm{R}}}{\mathcal{F}(Q,n_1) r_0^3} \frac{t_{\mathrm{KH}}}{t_M} < \int\limits_0^{\theta_{\max}} g(y(\theta))\, y(\theta) \sin\theta \, \mathrm{d}\theta , \tag{60}$$

replacing the simpler estimate (45). The left hand side Λ of (60) is the same as in (45) with $f = \mathcal{F}$ and shown in Fig. 3. All information about irradiation is contained in the integral on the right hand side of (60), the value of which depends on the function $g(y)$. The integral could be replaced by $2s\bar{y}g(\bar{y})$, where $\bar{y}$ is an adequate mean value of y over the illuminated fraction $s = (1-f_2)/2$ of the surface. In this context it is now important to note the following general properties of the function $g(y)$:

1) $\int\limits_0^{\infty} g(y)\, \mathrm{d}y = 1$,

since $G(0) = 1$, and $\sigma T_2^4 = F$ (i.e. $G = 0$) if irradiation is very strong ($F \to \infty$) and the flux from the stellar interior is completely blocked,

2) $g(y) \leq 1$ for positive albedos,

since T_2 increases monotonically with F, and

3) $\lim_{y\to\infty} g(y) = 0$,

a consequence of (1). Properties (1) and (2) are equivalent to the motivations (a)–(c) for the simplified ansatz in Sect. 5.1. Furthermore we know from numerical computations (Hameury 1995, private communication) and from the simple one-zone model of Ritter et al. (1995, 1996b) that g is a monotonically decreasing function of y and that for low-mass stars with $M \lesssim 0.6\mathrm{M}_\odot$, $g(y = 0) \approx 1$. From all these properties it follows that $g(y)$ is a rather steeply decreasing function, with $yg(y) = 0$ for $y = 0$ and $y \to \infty$, and that $yg(y) < 1$ for all y. In fact, the numerical computations show that $yg(y)$ attains a maximum value $\mathrm{Max}(yg(y)) \lesssim 0.5$ for y of order a few, and that the integral in (60) has a maximum value $\lesssim 0.25$. As in Sect. 5.1 this translates into a limiting mass, $M_2 \simeq 0.65\mathrm{M}_\odot$ (see Fig. 3), below which (60) cannot be fulfilled. Given the very general nature of the assumptions entering our model and the function g, we conclude that no irradiation–induced mass–transfer cycles can occur if $M_2 \lesssim 0.65\mathrm{M}_\odot$. A more detailed treatment of (60), using the actual value of the integral rather than an upper limit, shows that the condition is not satisfied near $M_2 = 0.2\mathrm{M}_\odot$ either (Ritter et al. 1996a).

6. ANGULAR MOMENTUM LOSSES MODULATED BY IRRADIATION

The last section shows that we cannot construct a satisfactory model of mass transfer cycles in CVs with orbital periods $\lesssim 5.5$ h by considering only the reaction of the companion's radius to irradiation. This is because for $M_2 \lesssim 0.65\mathrm{M}_\odot$ the thermal inertia of the secondary's convective envelope is too large for cycles to occur at all: irradiation cannot expand the star relative to its equilibrium radius more rapidly than the simultaneous relative increase of the Roche lobe, as is required for a local instability.

It is clear that this problem arises purely from properties of the secondary star and cannot be evaded by different assumptions about irradiation; those made in the two treatments given here are quite reasonable, and other schemes will give similar results. The italicised conclusion of Sect. 4 was that only irradiation is at all promising for driving cycles through radius variations. Hence we must look more widely than radius variations for the cause of mass transfer cycles. There are essentially three possibilities. We could abandon attempts to produce a limit cycle, and consider explicitly time–dependent radius variations (mathematically $K = K(t)$) such as might result from starspot cycles. This only throws the problem back to the origin of the latter cycles, and no promising model exists. We might consider instead the effects of variations of the stellar scale height H: however these occur on such short timescales (minutes) that is it difficult to see how they can be the basis for the long–term cycles we are interested in. Finally we may allow for variations in the angular momentum loss rate $\dot{J}$. This is fairly plausible if there is some contribution to $\dot{J}$ from magnetic stellar wind braking: we might expect that irradiation could increase the wind mass–loss rate, and indeed there are explicit models which assume precisely this (Tavani, Ruderman & Shaham 1989; Tavani 1991). This in itself does not necessarily increase $\dot{J}$, but the effect of irradiating the corona of the secondary may well be to increase the number of field lines contributing to the braking, thus raising $\dot{J}$. Alternatively it is conceivable that angular momentum loss from disc winds might also increase with the mass transfer rate, although the total losses from such winds are rather tightly limited, and they certainly cannot be important in the global evolution of CVs

(King & Kolb 1995).

For the moment we simply allow formally for coupled variations in $\dot{J}$ without speculating on their origin. We write the variations in the form

$$-\frac{\dot{J}}{J} = \frac{j(r,x)}{t_J} \,, \tag{61}$$

and as before regard t_J, the secular mean angular momentum loss timescale, as constant over the cycles. We repeat the analysis of Sect. 2, and again neglect terms of order ϵ. However in (4) we must now use (61) rather than $-\dot{J}/J = 1/t_J$, so (11) becomes

$$\frac{\mathrm{d}x}{\mathrm{d}\tau} = rx[j(r,x) + p(r,x) - x] \,, \tag{62}$$

while (12) remains unchanged:

$$\frac{\mathrm{d}r}{\mathrm{d}\tau} = \epsilon r \left[p(r,x) - \frac{x}{\lambda} \right] . \tag{63}$$

The fixed points of this pair of equations are easily found to be

$$x_0 = \frac{\lambda j}{\lambda - 1} \,, \tag{64}$$

$$p_0 = p(r_0, x_0) = \frac{j}{\lambda - 1} \,, \tag{65}$$

generalizing (13, 14). As before global properties of the system will be determined by the locus of $\dot{x} = 0$, which now becomes

$$j(r,x) + p(r,x) - x = 0 \,, \tag{66}$$

with slope

$$\frac{\mathrm{d}x}{\mathrm{d}r} = \frac{p_r + j_r}{1 - p_x - j_x} \,. \tag{67}$$

Clearly we can prove an extension to the italicised statement at the end of Sect. 4, i.e. that limit cycles require the *sum* $(p + j)$ to depend on x, with $p_x + j_x > 1$ at the fixed point.

To discover the main effects of allowing for variations of the angular momentum losses coupled to the transfer rate we consider the simplest possible case, in which these increase linearly with x, i.e.

$$j = 1 + lx, \quad l > 0 \,. \tag{68}$$

Formally, this is an example for a consequential angular momentum loss (CAML, cf Webbink 1985; King & Kolb, 1995): $\dot{J}/J$ is the sum of a $\dot{M}_2$–independent "systemic" component, represented by $1/t_J$, and the "consequential" component

$$\frac{\dot{J}_{\mathrm{CAML}}}{J} = l \; D_s \, \frac{\dot{M}_2}{M_2} \,. \tag{69}$$

As shown in King & Kolb (1995) stability against dynamical–timescale mass transfer requires $D = D_s(1 - l) > 0$, i.e. $l < 1$.

With (68) the fixed point in (64) becomes

$$x_0 = \frac{\lambda}{\lambda(1-l)-1} , \tag{70}$$

and $j_r = 0$ in (67). For $p(r, x)$ we take the approximate analytic form (38), so that

$$p_x = \frac{sf\rho}{2x_c} r^3 \mathrm{sech}^2 \frac{x}{x_c} \approx \frac{sf\rho}{2x_c} \mathrm{sech}^2 \frac{x}{x_c} \tag{71}$$

since $r \approx 1$ in all cases. It is then clear that once again the curve (66) has stable (unstable) branches where $1 - p_x - j_x$ is positive (negative), with a turning point where this combination vanishes. From (71) the corresponding value of x is $x_{\rm turn}$, now given by

$$\cosh^2 \frac{x_{\rm turn}}{x_c} = \frac{sf\rho}{2x_c(1-l)} . \tag{72}$$

Of course we recover the earlier case of pure irradiation if $l \to 0$ (cf (45)). In that case we found $x_0 > x_{\rm turn}$ for $M_2 \lesssim 0.65 \mathrm{M}_\odot$, so that the fixed point was on the stable branch of the $\dot{x} = 0$ curve, and there was no limit cycle. With now $l \neq 0$ we evidently require $l < 1$ if there is to be any stable branch at all, consistent with (69); but if l approaches unity from below, $x_{\rm turn}$ becomes very large, while $x_0 \to -\lambda$ remains finite. We see that angular momentum losses with this property imply

$$x_{\rm turn} > x_0 , \tag{73}$$

so that the fixed point is now always on an unstable part of the $\dot{x} = 0$ curve. This removes the main difficulty encountered in Sect. 5 in driving limit cycles by radius variations alone and greatly increases the amplitude of the mass transfer variations. Note that the requirement that l should approach 1 is not severe, as it demands only that the angular momentum losses should increase by a factor of 2 at the adiabatic mass transfer rate $x = 1$ compared with $x = 0$. It thus appears that allowing for the variation of angular momentum losses upon irradiation may provide the key to making the mass transfer cycles effective.

7. CONCLUSIONS

In this paper we have given a general formulation allowing a global analysis of mass transfer variations on timescales short compared with the secular evolution timescale but longer than dynamical. We have shown that radius variations can drive limit cycles only if the radius is sensitive to the instantaneous mass transfer rate: the only plausible mechanism ensuring this appears to us to be irradiation of the companion star. Explicit modelling of the resulting radius variations however shows that limit cycles occur only for companion masses $\gtrsim 0.65 \mathrm{M}_\odot$. Allowing for simultaneous variations in the angular momentum loss rate from the binary completely alters this picture: quite modest increases in these losses extend limit–cycle behaviour to all companion masses and greatly increase the amplitudes of the cycles. It appears then that the long–sought mass transfer cycles involve variations of *both* the companion radius *and* the angular momentum loss rate, the former providing the necessary hysteresis through the thermal inertia of the companion's envelope. However a definite conclusion must await an understanding of how angular momentum losses depend on the prevailing mass transfer rate. Given this, we may be closer to working out how the various CV subtypes are related.

UK and HR thank Zhongyong Zhang for helpful discussions. ARK thanks the Max–Planck–Institut für Astrophysik for warm hospitality during a productive stay in July–August 1994.

This work was partially supported by the U.K. Science and Engineering Research Council (now PPARC); and by NASA grants NAGW-2447 and NAG5-2777, and NSF grant AST-9020855 to LSU. ARK acknowledges support as a PPARC Senior Fellow. We particularly thank the anonymous referee for a very careful and perceptive reading of the paper, which led to many improvements.

REFERENCES

Glendinning, P., 1994, Stability, Instability and Chaos, (Cambridge: CUP), Ch. 5

Hameury J.M., King A.R., Lasota J.P., & Ritter H. 1988, MNRAS, 231, 535

Hjellming M.S. 1989, Ph.D. thesis, University of Illinois

King, A.R., 1988, QJRAS 29, 1

King, A.R., 1995, in: Cataclysmic Variables, A. Bianchini, M. Della Valle, & M. Orio (eds), Kluwer, p. 523

King, A.R., Frank, J., Kolb, U., & Ritter, H. 1995, ApJ, 444, L40

King A.R., & Kolb U., 1995, ApJ 439, 330

Kolb U., & Ritter H. 1992, A&A, 254, 213

Minorsky, N., 1962, Nonlinear Oscillations, (Princeton: Van Nostrand), Ch. 3

Paczyński B., & Sienkiewicz R., 1981, ApJ 248, L27

Patterson J., 1984, ApJ Suppl. 54, 443

Rappaport S., Verbunt F. & Joss P.C., 1983, ApJ, 275, 713

Ritter H., 1988, A&A 202, 93

Ritter H., Zhang Z., & Hameury J.M., 1996a, in: Cataclysmic Variables and Related Objects, IAU Coll. 158, A. Evans, J.H. Wood (Eds.), Kluwer, in press

Ritter H., Zhang Z., & Kolb U., 1996b, in: Compact Stars in Binaries, IAU-Symp. 165, E.P.J. van den Heuvel (Ed.), in press

Ritter H., Zhang Z., & Kolb U., 1995, in: Cataclysmic Variables, A. Bianchini, M. Della Valle, & M. Orio, Kluwer, p. 479

Stehle,R., Ritter, H., & Kolb, U. 1996, MNRAS, in press

Tavani, M., 1991, Nature, 351, 39

Tavani, M., Ruderman, M., & Shaham, J., 1989, ApJ, 342, L39

Tout C.A., & Pringle J.E., 1992, MNRAS 256, 269

Warner B., 1987, MNRAS 227, 23

Webbink, R.F., 1985, in Interacting Binary Stars, ed. J. Pringle & R.A. Wade (Cambridge: Cambridge Univ. Press), 39

This preprint was prepared with the AAS LaTeX macros v4.0.

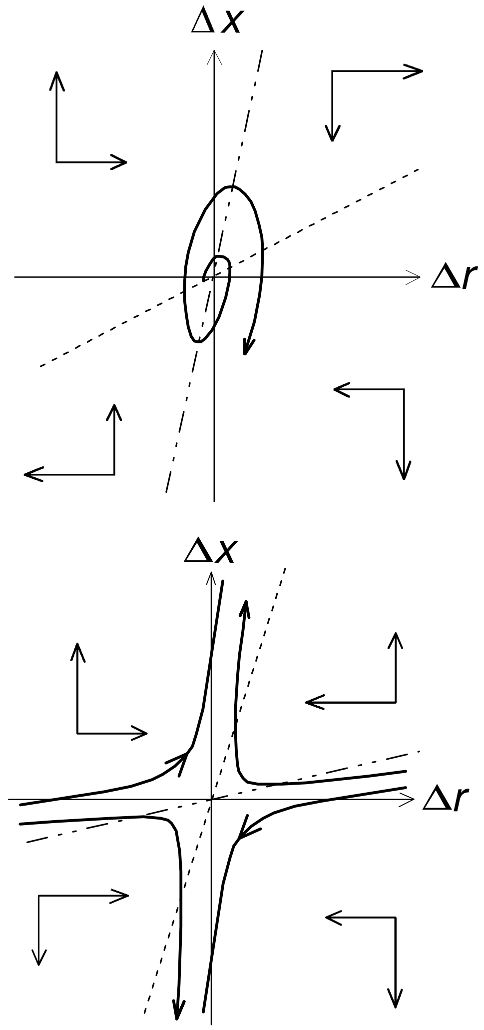

Fig. 1.— Local phase plane $(\Delta r, \Delta x)$ representing small deviations from the stationary values of the dimensionless secondary radius and mass transfer rate. The fixed point is at the origin. The lines $\dot{\Delta r} = 0$ (shown dashed), and $\dot{\Delta x} = 0$ (shown dot–dot–dashed) divide the neighbourhood of the fixed point into four regions. In each of these the system point moves as shown by the directions of the arrows. (a) In this case the fixed point given by the intersection of the two lines is an unstable focus, so the system moves away from it as shown. Physically this case corresponds to (subcritical) antidamping of the mass transfer rate as a function of the radius, i.e. a growing oscillation. As we move around the fixed point, the arrow pattern rotates exactly once, in the same sense as our rotation, showing the the Poincaré index of the unstable focus is $+1$. (b) Local phase plane $(\Delta r, \Delta x)$ for the case of a saddle point. The system point moves away from the fixed point as shown. As we move around the fixed point the arrow pattern rotates exactly once, but in the opposite sense, showing that the Poincaré index of the saddle point is -1.

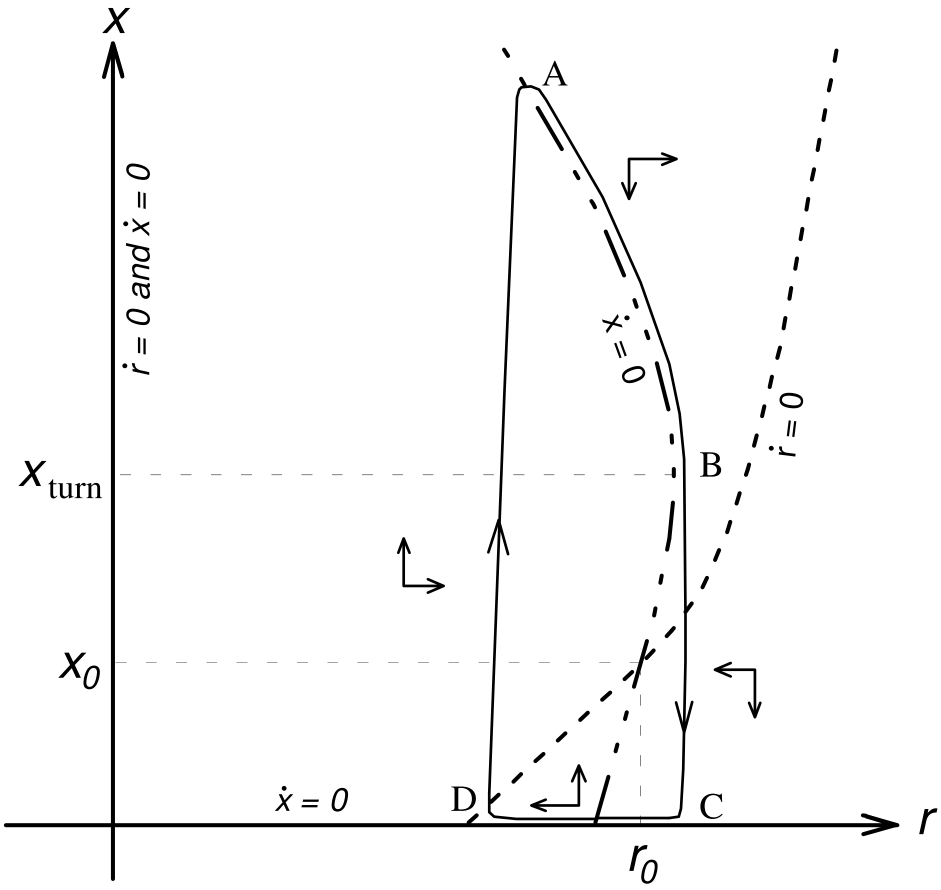

Fig. 2.— Global phase plane behaviour for the ODE system (11, 12). The two critical curves where $\dot{x} = 0$ (dot-dot-dashed) and $\dot{r} = 0$ (dashed) are shown for a typical $p(r, x)$. As in Fig. 1 these curves intersect at the fixed point (r_0, x_0) and divide the (r, x) plane into four regions in which the motion of the system point is indicated by the arrows. Away from the curves $\dot{r} = 0, \dot{x} = 0$ the motion in x is much more rapid than in r, so the system point moves effectively vertically. The system point is attracted to branches of the $\dot{x} = 0$ curve with negative slope, and repelled from those with positive slope. Here the $\dot{x} = 0$ curve changes from negative to positive slope at the turning point $x = x_{\rm turn}$, so the branch $x > x_{\rm turn}$ is stable and that with $x < x_{\rm turn}$ is unstable. On stable branches the system point tries to move in x towards the fixed point. Here the fixed point (r_0, x_0) lies on an unstable branch (i.e. $x_0 < x_{\rm turn}$ so the system point is repelled from it). Since an attracting branch of the $\dot{x} = 0$ curve is available above this point, and $x = 0$ is approached only exponentially slowly, the system is trapped in the neighborhood of the fixed point and moves clockwise around it in a limit cycle ABCD. Physically this implies small amplitude radial variations and large amplitude mass transfer variations.

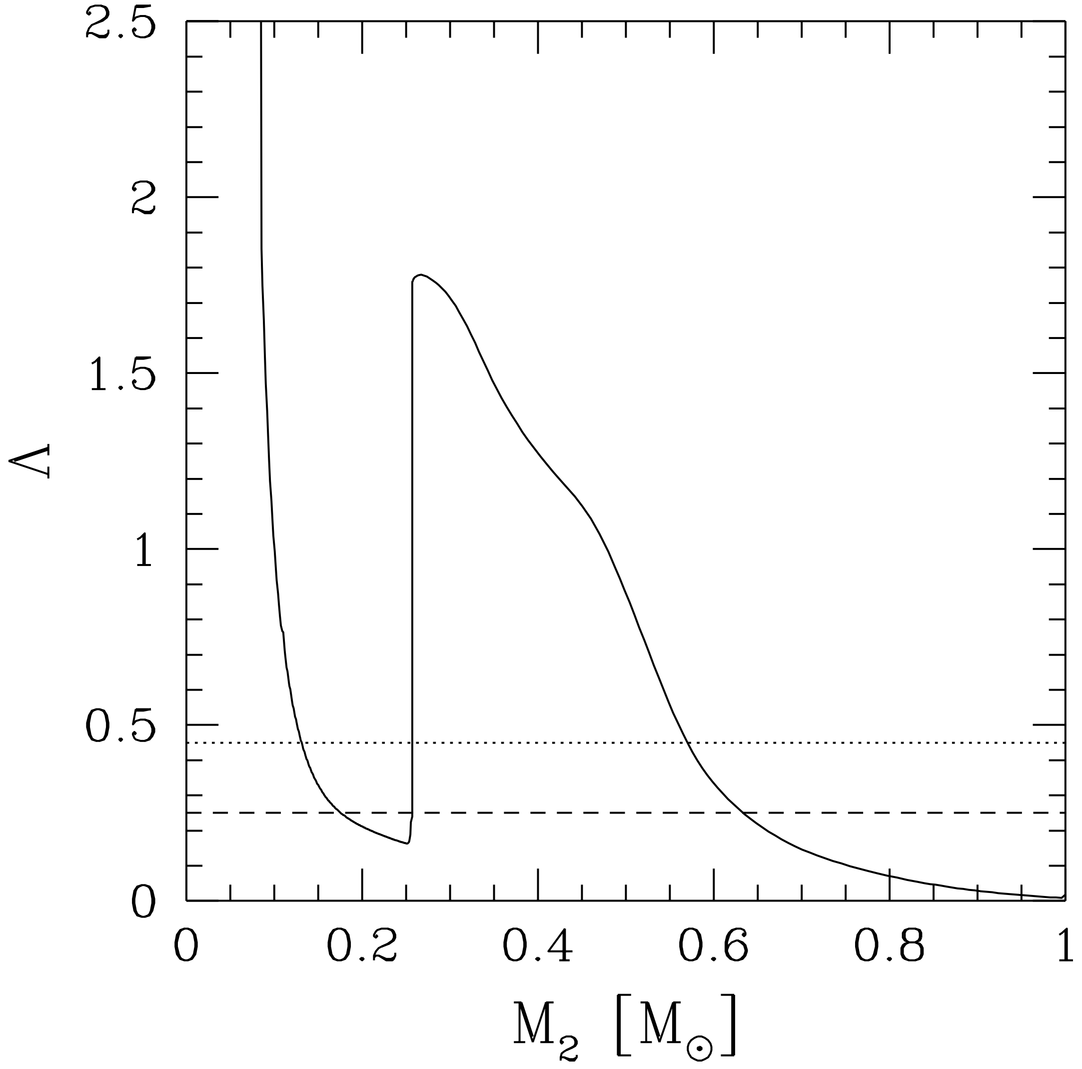

Fig. 3.— The necessary condition for occurrence of limit cycles ((45) or (60)) is satisfied when the l.h.s. Λ of these inequalities (solid curve) falls below the r.h.s. Global upper limits for the r.h.s. of (45) and (60) are shown as dotted and dashed lines, respectively. This demonstrates that pure irradiation models are unlikely to work for companions $M_2 \lesssim 0.65\mathrm{M}_\odot$. Cycles do not occur near $M_2 = 0.2\mathrm{M}_\odot$ despite the fact that Λ is below the upper limit to the integral, as shown by a more detailed treatment (Ritter et al. 1996a).

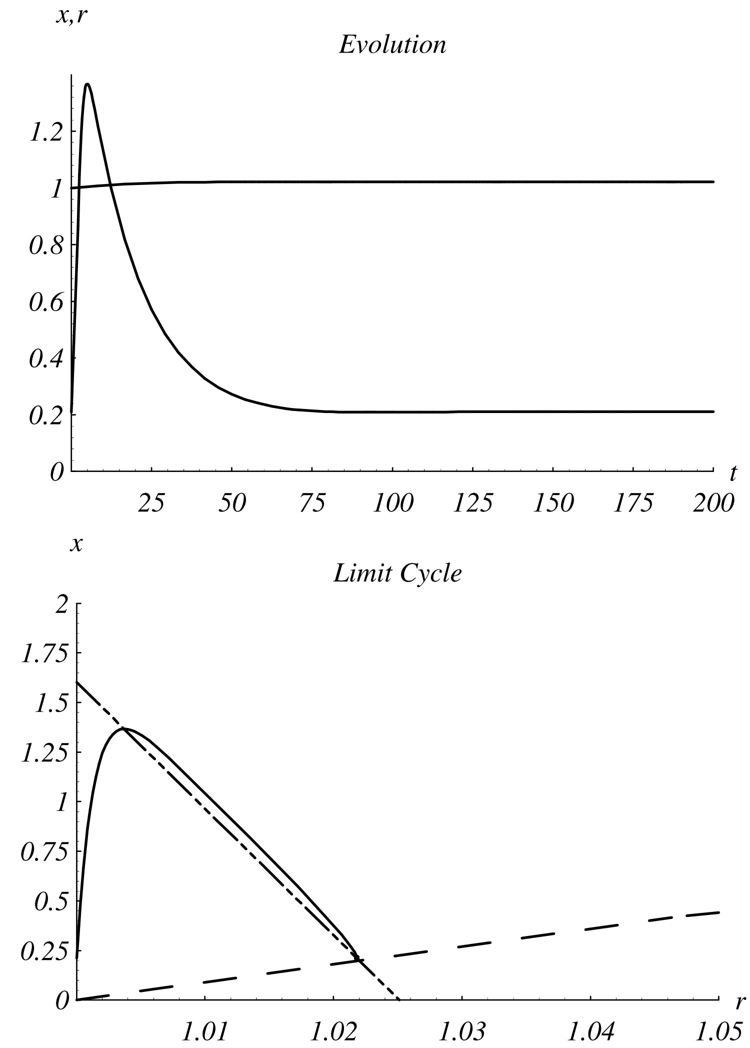

Fig. 4a

Fig. 4.— Four time evolutions calculated by integrating equations (11) and (12) from an arbitrarily chosen initial state with $p(r, x)$ given by (38). The critical curves where $\dot{x} = 0$ (dot-dot-dashed) and $\dot{r} = 0$ (dashed) intersect at the fixed point (r_0, x_0). The parameters used for the integrations are as follows: for all cases: $s = 0.5$, $\zeta_e = 1.0$, $\zeta_{\rm R} = 2q - 5/3$, and $\epsilon = 0.0002$; and for Stable Case a: $q = 0.7$, $x_c = 5.0$, $\zeta_s = 0.0$, and $f\rho/2 = 3.89$; for Unstable Case b: $q = 0.8$, $x_c = 5.0$, $\zeta_s = 0.5$, and $f\rho/2 = 23.3$; for Stable Case c: $q = 0.8$, $x_c = 10$, $\zeta_s = 0.0$, and $f\rho/2 = 11.67$; and for Unstable Case d: $q = 0.8$, $x_c = 5.0$, $\zeta_s = 0.5$, and $f\rho/2 = 11.67$.

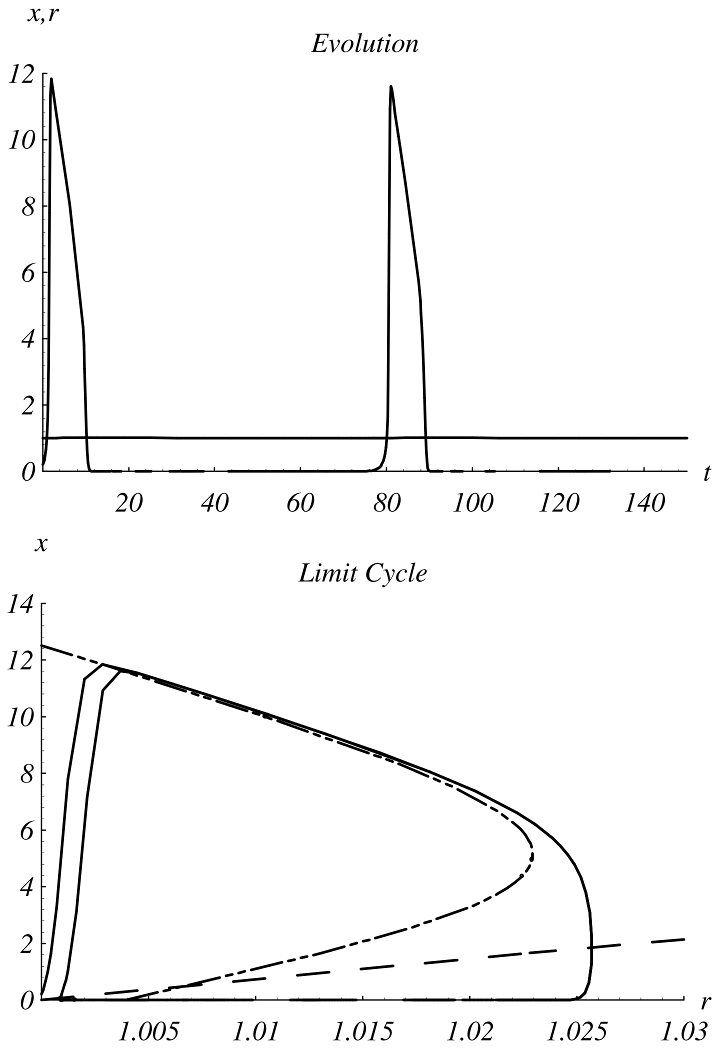
x,r
Evolution
12
10
8
6
4
2
0
t
20
40
60
80
100
120
140
x
Limit Cycle
14
12
10
8
6
4
2
0
r
1.005
1.01
1.015
1.02
1.025
1.03

Fig. 4b

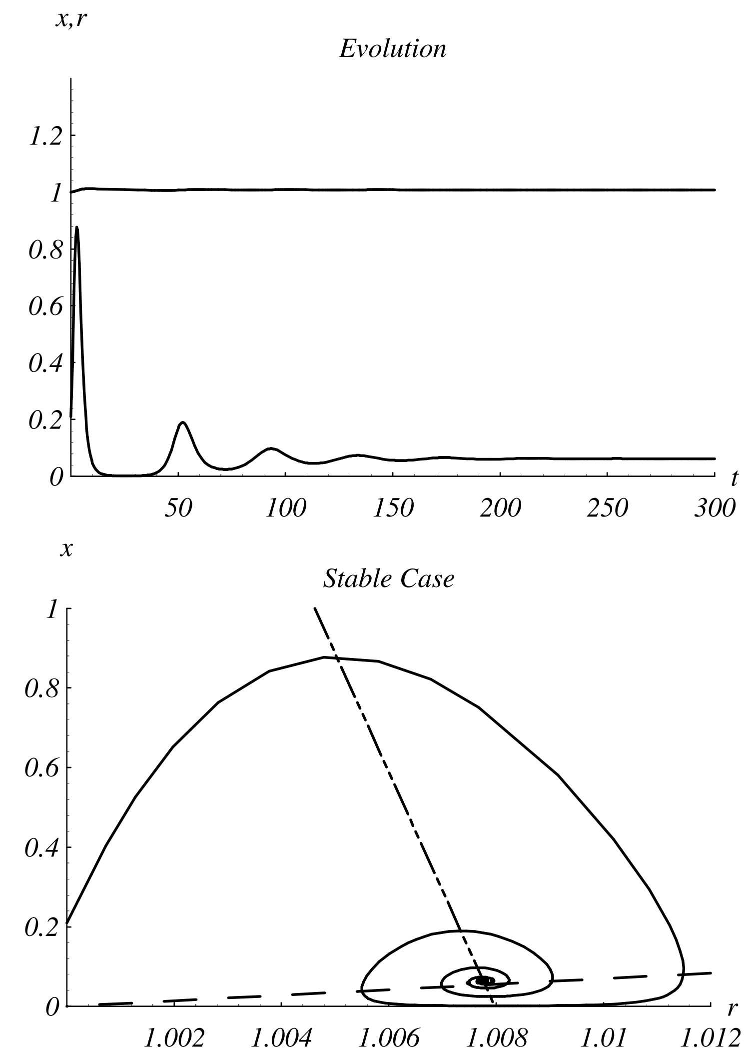
x,r
Evolution
1.2
1
0.8
0.6
0.4
0.2
0
t
50
100
150
200
250
300
x
Stable Case
1
0.8
0.6
0.4
0.2
0
r
1.002
1.004
1.006
1.008
1.01
1.012

Fig. 4c

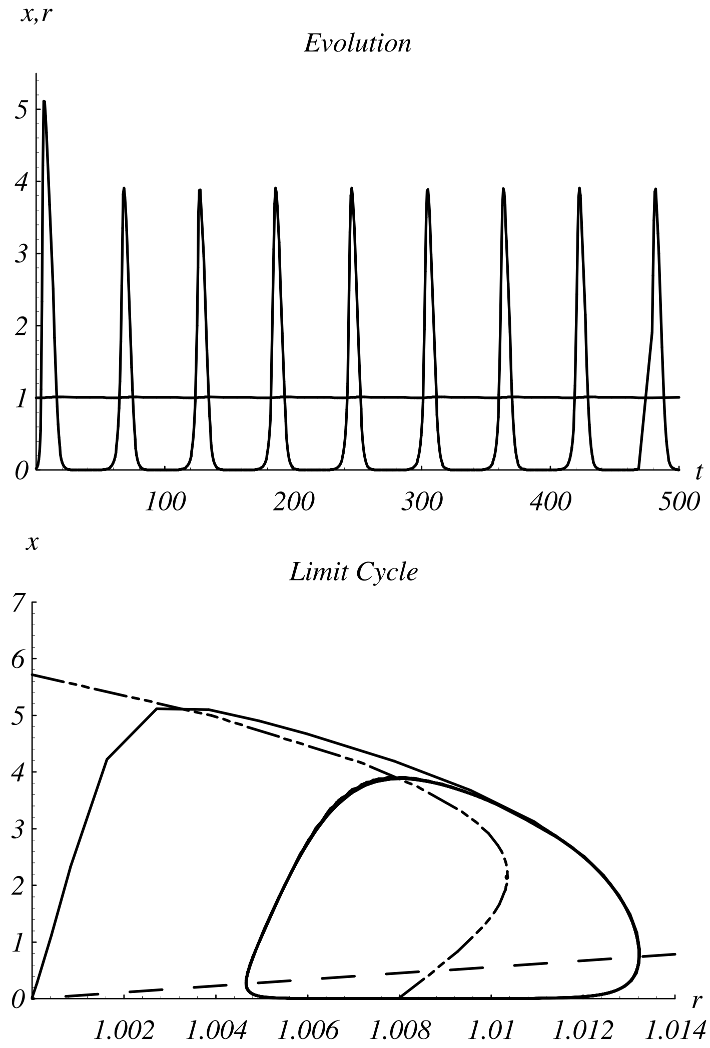

x,r
Evolution
5
4
3
2
1
0
t
100
200
300
400
500
x
Limit Cycle
7
6
5
4
3
2
1
0
r
1.002
1.004
1.006
1.008
1.01
1.012
1.014

Fig. 4d

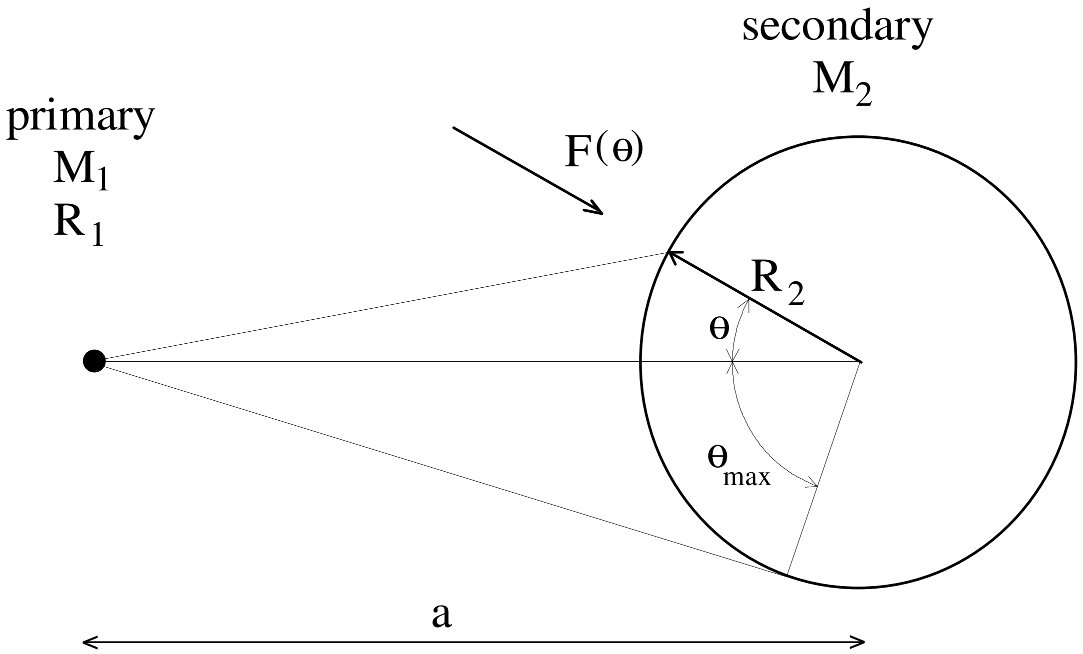

Fig. 5.— Schematic diagram showing a spherical companion irradiated by a point source and illustrating the definitions of quantities entering equations (49, 50). Note that $F(\theta)$ is the flux normal to the stellar surface.

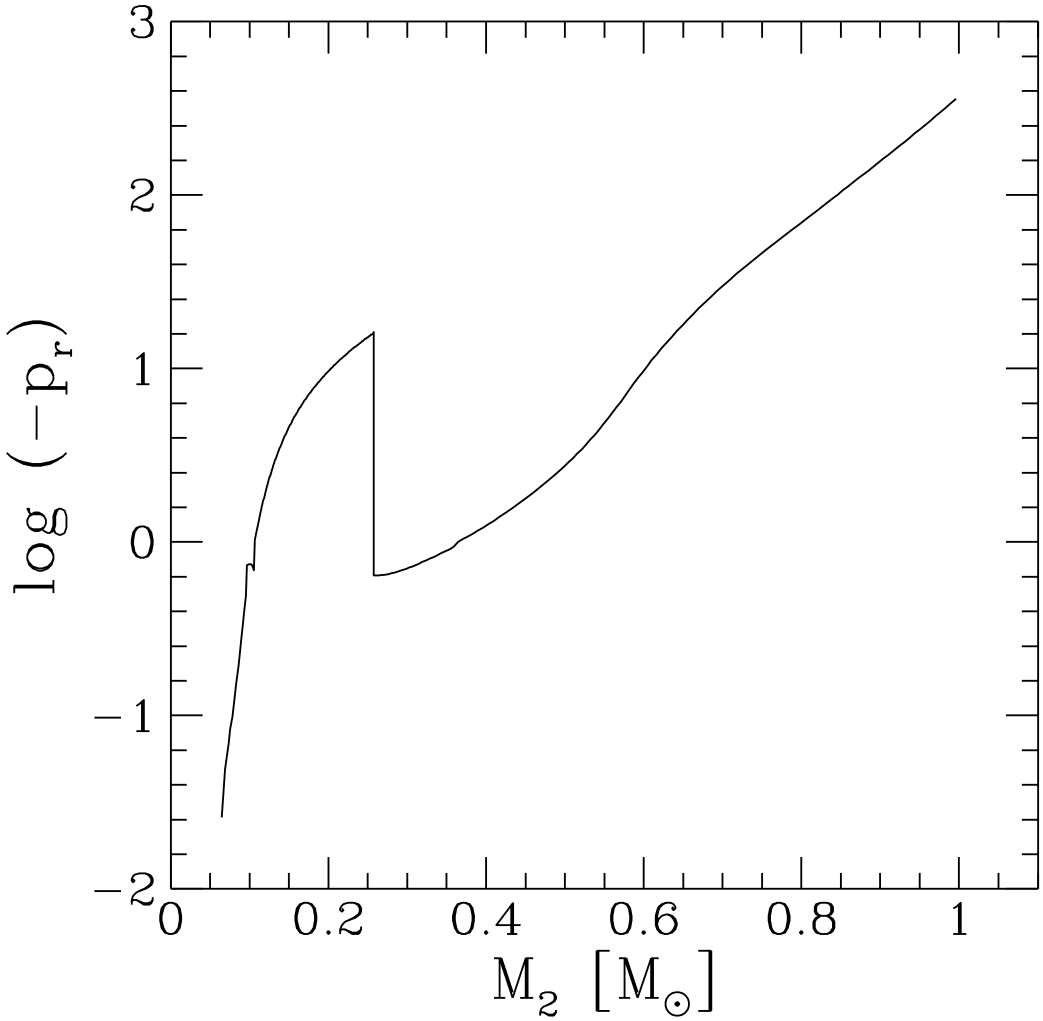

Fig. 6.— Behaviour of p_r obtained by numerical differentiation as a function of secondary mass M_2 along a standard evolutionary sequence for a cataclysmic variable, taken from Kolb & Ritter (1992). Note that ω is real when $p_r < 0$.